

Photophysical properties of polyads containing a fluorescein moiety

Aimin Song *, Hong Zhang, Manhua Zhang, Tao Shen

Institute of Photographic Chemistry, Chinese Academy of Sciences, Beijing, 100101, People's Republic of China

Received 12 November 1998; accepted 12 December 1998

Abstract

A series of dyads, triads and tetrads containing fluorescein as photosensitizer, carbazole as electron donor, viologen and anthraquinone as electron acceptors, and their model compounds were synthesized and characterized. Their absorption spectra, fluorescence spectra, fluorescence lifetimes, the free energy changes of photoinduced intramolecular electron transfer and recombination in methanol were measured and estimated. In all the polyads, the fluorescence of fluorescein is strongly quenched in methanol. The quenching by carbazole and anthraquinone is dominantly a dynamic electron transfer process, while viologen readily forms a non-emitting complex with fluorescein in polyads, possibly due to its double positive charges. When fluorescein in the triads and tetrads is excited, the primary photoinduced intramolecular interaction process is mainly electron transfer from carbazole to fluorescein. Estimation of the free energy changes of the electron transfer reactions indicates that in the triads and tetrads, after the initial charge separation, the subsequent electron transfer processes can occur, and longer-lived charge-separated products can eventually be obtained. © 1999 Elsevier Science Ltd. All rights reserved.

Keywords: Fluorescein; Carbazole; Anthraquinone; Viologen; Polyads; Photoinduced electron transfer

1. Introduction

Over the past years, significant emphasis has been put on the development and understanding of photoinduced electron transfer reactions as a method of converting and storing solar energy [1]. Covalently linked multicomponent models have been reported, in which the dependence of the electron transfer rate constant on the donor-acceptor distance, orientation, free energy of reaction and electronic coupling has been studied

[1]. Fluorescein **1** (Fig. 1) is an important xanthene dye with a large variety of technical applications due to its high quantum yield of fluorescence, intense absorption in the visible range and appropriate redox potentials [2].

Fluorescein contains two active groups, viz., the carboxyl group and the hydroxyl group, which can link donors or acceptors to form multicomponent compounds [3,4]. In the present study, a series of dyads, triads and tetrads containing fluorescein (FL) as the photosensitizer (S), carbazole (CZ) as the electron donor (D), viologen bromide (VL) (1,1'-dialkyl-4,4'-bipyridinium dibromide) and anthraquinone (AQ) as electron acceptors (A),

* Corresponding author. Tel: +86-10-64888156; fax: +86-10-64879375; e-mail: g214@ipc.ac.cn

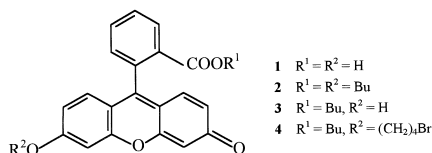


Fig. 1. Structural formula of fluorescein and its alkyl derivatives.

were designed and synthesized. The processes of intramolecular electron transfer and formation of a non-emitting complex were studied by comparison with a model compound, i.e. the dibutyl derivative of fluorescein **2**. The relationship between photophysical properties and the structural features in the polyads was also investigated.

2. Experimental

2.1. Syntheses

Dibutyl derivative of fluorescein **2** and the butyl ester of fluorescein **3**, 9-(4-bromo)butyl-carbazole, and 2-bromomethylantraquinone were prepared according to the procedures described in Refs. [5]–[7], respectively. The polyads were synthesized as shown in Fig. 2.

The spectral data of the polyads are as follows:

The dyad consisting of carbazole and fluorescein
9. λ_{\max} (methanol)/nm 454, 482. ν_{\max} (KBr)/ cm^{-1} 1709, 1637, 1592. $\delta_{\text{H}}[(\text{CD}_3)_2\text{SO}]$ 0.92 (t, 3H), 1–2 (m, 8H), 3.90 (t, 2H), 4.08 (t, 2H), 4.25 (t, 2H), 6.24 (s, 1H), 6.40 (d, 1H), 6.80 (m, 3H), 7.14 (s, 1H), 7.18 (t, 2H), 7.42 (t, 2H), 7.45 (d, 2H), 7.49 (d, 1H), 7.74 (t, 1H), 7.84 (t, 1H), 8.13 (m, 3H). m/z (FAB) 610 ($M+1$)⁺.

The dyad consisting of fluorescein and anthraquinone
10. λ_{\max} (methanol)/nm 454, 482. ν_{\max} (KBr)/ cm^{-1} 1707, 1668, 1636, 1591, 1513. $\delta_{\text{H}}[(\text{CD}_3)_2\text{SO}]$ 0.66 (t, 3H), 1–2 (m, 4H), 3.90 (t, 2H), 5.51 (s, 2H), 6.26 (s, 1H), 6.41 (d, 1H), 6.80–6.90 (m, 2H), 7.06 (d, 1H), 7.38 (s, 1H), 7.51 (d, 1H), 7.79 (t, 1H), 7.87 (t, 1H), 7.92–7.98 (m, 2H), 8.01 (d, 1H), 8.18 (d, 1H), 8.22–8.26 (m, 2H), 8.29 (d, 1H), 8.30 (s, 1H). m/z (FAB) 610 (M)⁺.

The dyad consisting of fluorescein and viologen
11. λ_{\max} (methanol)/nm 456. ν_{\max} (KBr)/ cm^{-1} 1725, 1588. $\delta_{\text{H}}[(\text{CD}_3)_2\text{SO}]$ 0.66 (t, 3H), 0.92 (t, 3H), 1.1–2.0

(m, 12H), 3.90 (t, 2H), 4.06 (t, 2H), 4.28 (t, 2H), 4.31 (t, 2H), 6.19 (s, 1H), 6.7–7.0 (m, 3H), 7.17 (d, 1H), 7.24 (s, 1H), 7.39 (d, 1H), 7.77 (t, 1H), 7.87 (t, 1H), 8.04 (d, 1H), 8.76 (d, 4H), 9.45 (d, 4H). m/z (FAB) 656 (M)⁺.

The triad consisting of carbazole, fluorescein and anthraquinone
12. λ_{\max} (methanol)/nm 454, 482. ν_{\max} (KBr)/ cm^{-1} 1704, 1668, 1635, 1592, 1541, 1514. $\delta_{\text{H}}[(\text{CD}_3)_2\text{SO}]$ 1–2 (m, 4H), 3.88 (t, 2H), 4.15 (t, 2H), 5.52 (s, 2H), 6.24 (s, 1H), 6.38 (d, 1H), 6.79–6.98 (m, 3H), 7.14 (t, 2H), 7.33 (s, 1H), 7.44–7.47 (m, 4H), 7.49 (d, 1H), 7.76 (t, 1H), 7.87 (t, 1H), 7.88–7.98 (m, 3H), 8.06 (d, 2H), 8.09–8.13 (m, 3H), 8.22 (d, 1H), 8.29 (s, 1H). m/z (FAB) 775 (M)⁺.

The triad consisting of carbazole, fluorescein and viologen
13. λ_{\max} (methanol)/nm 456. ν_{\max} (KBr)/ cm^{-1} 1710, 1591. $\delta_{\text{H}}[(\text{CD}_3)_2\text{SO}]$ 0.96 (t, 3H), 1.0–2.2 (m, 12H), 3.94 (t, 2H), 4.16 (t, 2H), 4.28 (t, 2H), 4.70 (t, 2H), 4.78 (t, 2H), 6.24 (s, 1H), 6.42 (d, 1H), 6.82 (m, 3H), 7.18 (m, 3H), 7.42 (t, 2H), 7.48 (m, 3H), 7.77 (t, 1H), 7.87 (t, 1H), 8.11 (d, 1H), 8.13 (d, 2H), 8.79 (d, 4H), 9.40 (d, 4H). m/z (FAB) 821 (M)⁺.

The tetrad consisting of carbazole, fluorescein, viologen and anthraquinone
14. λ_{\max} (methanol)/nm 456, 484. ν_{\max} (KBr)/ cm^{-1} 3463, 3043, 1705, 1668, 1635, 1592, 1514. $\delta_{\text{H}}[(\text{CD}_3)_2\text{SO}]$ 0.8–2.0 (m, 8H), 3.90 (t, 2H), 4.01 (t, 2H), 4.16 (t, 2H), 4.73 (t, 2H), 6.05 (s, 2H), 6.30 (s, 1H), 6.42 (d, 1H), 6.79 (d, 1H), 6.86 (d, 1H), 6.98 (d, 1H), 7.15 (d, 2H), 7.30–7.45 (m, 5H), 7.49 (d, 1H), 7.76 (t, 1H), 7.87 (t, 1H), 8.06 (d, 2H), 8.09–8.13 (m, 3H), 8.15–8.42 (m, 3H), 8.44–9.00 (m, 8H), 9.61 (d, 4H). m/z (FAB) 989 (M)⁺.

2.2. Physical measurement and instrumentation

Solvents for all spectroscopic experiments were dried and re-distilled before used. UV-Vis absorption spectra were recorded on a Shimadzu UV-160A spectrophotometer. Fluorescence spectra were obtained on a Hitachi MPF 4F spectrofluorimeter. Samples for fluorescence measurements were contained in 1-cm cuvettes. The emission was measured 90° to the excitation beam. Fluorescence quantum yields were determined by integrating the digitized emission spectra from 330

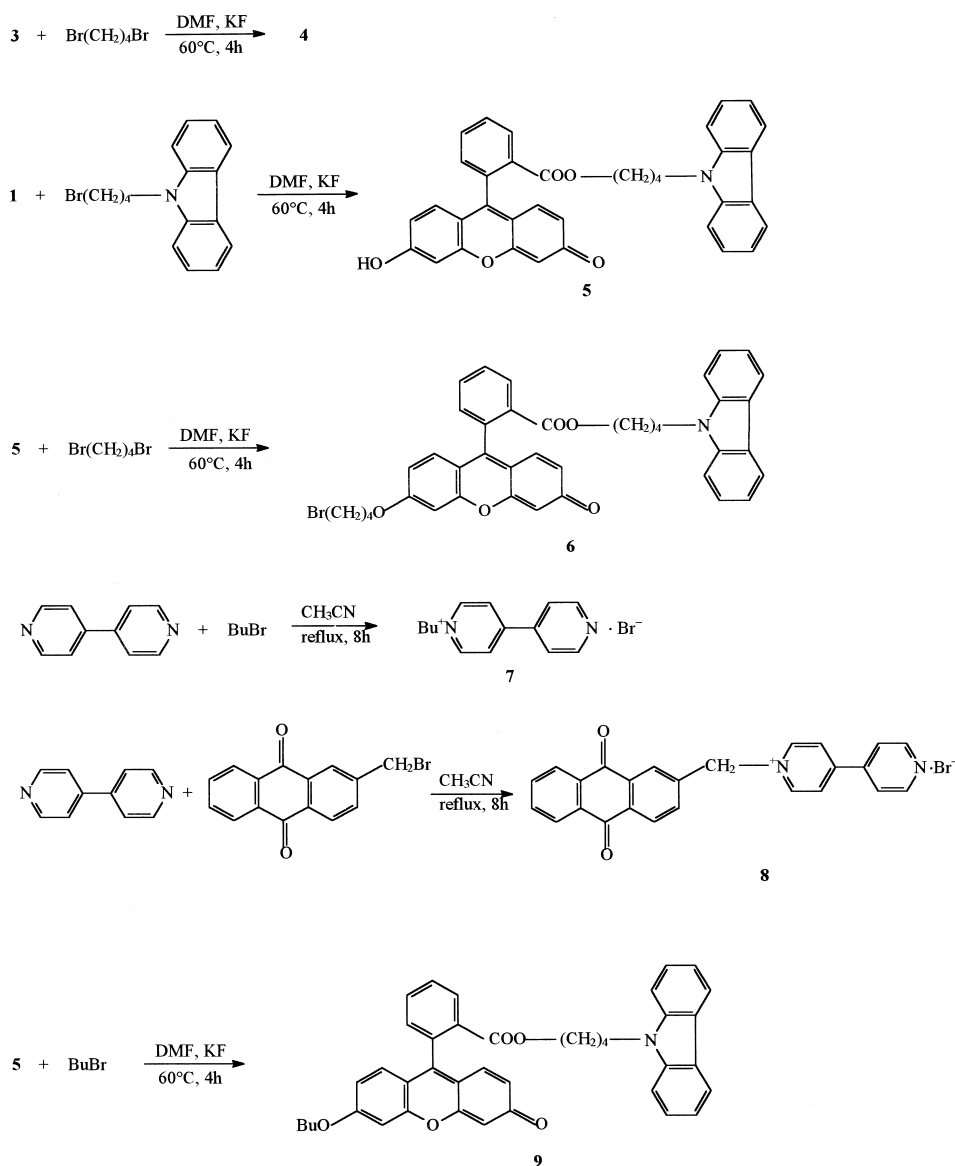


Fig. 2. Synthesis pathways of polyads.

to 800 nm and referring to fluorescein in methanol ($\Phi_f = 0.93$) [2]. The redox potentials of the model compounds were measured by cyclic voltammetry with pyrolytic graphite as the working electrode, platinum bridged by saturated KCl solution as the counter-electrode and Ag/AgCl (saturated KCl) as the electrolyte for a solution of 10^{-4} M in methanol. The singlet energy was determined from the overlap between the normalized absorption and

emission spectra [8]. Fluorescence lifetimes were determined using an HORIBA NAES-1100 single-photon counting apparatus.

2.3. Calculation

The free energy changes (ΔG) of photoinduced electron transfer reactions can be calculated with the Rehm–Weller equation [9]:

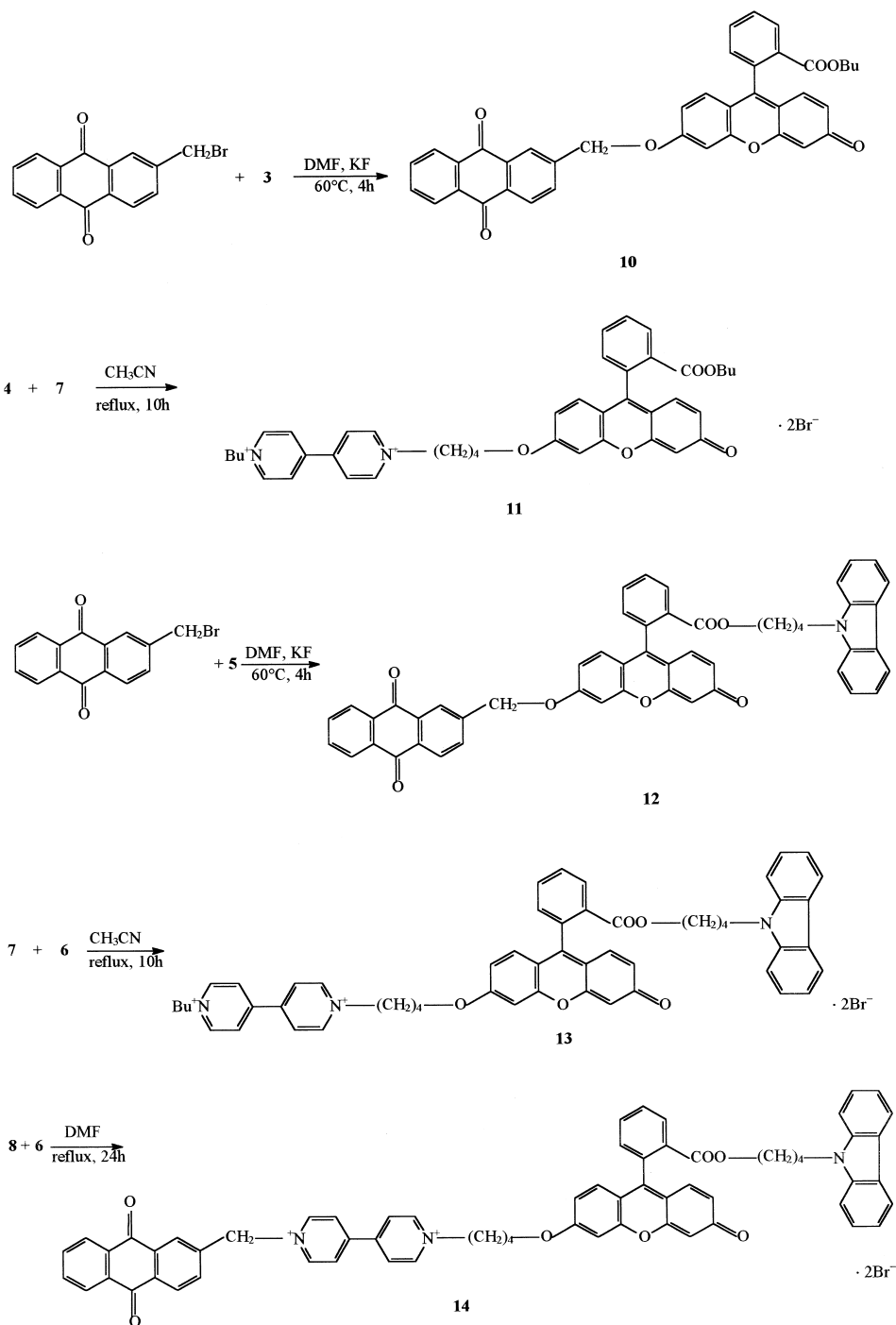


Fig. 2. cont.

$$\Delta G = E_O(D) - E_R(A) - E_S - C$$

In the polyads, the free energy changes of the further electron transfer reactions after the primary reaction are calculated as the following [10]:

$$\Delta G = E_O(D) - E_R(A)$$

and the free energy changes (ΔG^r) of reversed dark recombination reactions by [10]:

$$\Delta G^r = E_R(A) - E_O(D)$$

where $E_O(D)$ is the oxidation potential of the donor, $E_R(A)$ is the reduction potential of the acceptor, E_S is the singlet state energy of the sensitizer and C is the solubilizing energy of $D^{+\bullet}A^{-\bullet}$, which can usually be regarded as 0.06 eV or 1.4 kcal mol⁻¹ in polar solvents [11].

In the polyads, the fluorescence of photosensitizer can be quenched by the donors or acceptors. The fluorescence quenching efficiency can be obtained from the following equations:

1. Total quenching efficiency (Φ_Q). $\Phi_Q = 1 - \Phi_F/\Phi_{F,0}$.
2. Dynamic quenching efficiency (Φ_D). $\Phi_D = 1 - \tau_F/\tau_{F,0}$.
3. Static quenching efficiency (Φ_S). $\Phi_S = \Phi_Q - \Phi_D$.
4. Equilibrium constant of the intramolecular complex (K_C). If the fluorescence quenching is all due to the non-emitting intramolecular complex formation, $K_C = \Phi_{F,0}/\Phi_F - 1$; if there is another dynamic process to quench

fluorescence, the dynamic part should be subtracted and $K_C = \Phi_{F,0}/\Phi_F - \tau_{F,0}/\tau_F$ [12].

where $\Phi_{F,0}$ and $\tau_{F,0}$ represent the fluorescence quantum yield and fluorescence lifetime of the model compound, respectively, and where Φ_F and τ_F represent the fluorescence quantum yield and fluorescence lifetime of the polyads.

3. Results and discussion

3.1. Energetics

We selected the dibutyl derivative of fluorescein **2**, 9-butylcarbazole, 2-methylantraquinone and butyl viologen bromide (1,1'-dibutyl-4,4'-bipyridinium dibromide) as model compounds of the chromophores in polyads. The singlet state energy and the redox potentials of the model compounds are given in Table 1.

Table 1 shows that the singlet state energy of **2** is less than that of carbazole or anthraquinone or viologen, so that when fluorescein is excited, there will be no energy transfer in the polyads.

The calculated results of the free energy changes of electron transfer between the electron donors and acceptors in the polyads are given in Table 2.

3.2. Absorption and fluorescence spectra

The absorption spectra of the polyads containing viologen and the model compounds **2** in methanol are shown in Fig. 3 and those of the other polyads

Table 1
Singlet state energy and redox potentials of model compounds

Compound	E_S/eV^a	$E_O(D^{+\bullet}/D)\text{ eV}^b$	$E_R(A^{-\bullet}/A)\text{ eV}^c$
Dibutyl derivative of fluorescein 2	2.42	0.90	-1.20
9-Butyl-carbazole	3.60	1.10	—
2-Methyl-anthraquinone	2.88	—	-0.96
Butyl viologen bromide	4.16	—	-0.44

^a E_S is the singlet state energy of the sensitizer.

^b $E_O(D)$ is the oxidation potential of the donor.

^c $E_R(A)$ is the reduction potential of the acceptor.

Table 2

Calculated results of the free energy changes of electron transfer between donors and acceptors

D-A pair	$\Delta G^f/\text{eV}^a$	$\Delta G^r/\text{eV}^b$
FL(S, A)-CZ(D)	-0.19	-2.30
FL(S, D)-AQ(A)	-0.63	-1.86
FL(S, D)-VL(A)	-1.15	-1.34
FL ⁻ (D)-AQ(A)	-0.24	0.24
FL ⁻ (D)-VL(A)	-0.76	0.76
FL ⁺ (A)-CZ(D)	0.20	-0.20
AQ ⁻ (D)-VL(A)	-0.52	0.52
VL ⁻ (D)-AQ(A)	0.52	-0.52

^a ΔG^f is the free change of forward electron transfer reaction.

^b ΔG^r is the free energy change of reversed dark recombination reaction.

and their model compounds are shown in Fig. 4. The fluorescence spectra of the polyads and model compound **2** in methanol, when fluorescein was excited at 460 nm, are shown in Fig. 5. From Fig. 5, it can be seen that the fluorescence of fluorescein in the polyads is strongly quenched. The calculated results of fluorescence quenching efficiency are listed in Table 3.

In Fig. 3, the absorption spectra of fluorescein in the polyads containing viologen, dyad **11**, triad **13** and tetrad **14**, are broadened to some extent compared with that of the model compound **2**. Correspondingly, the emission band of fluorescein

in the polyads containing viologen shifts slightly to longer wavelength in Fig. 5. This indicates that there exists an intramolecular static interaction between fluorescein and viologen in the polyads. However, the static interaction obviously reduces in the order of dyad, triad and tetrad, and can be neglected in tetrad **14**. This may result from the enhanced spatial hindrance caused by the other attached groups in the polyads.

In Fig. 4, the absorption spectra of the other polyads are nearly identical with the sum of the spectra of the unlinked chromophores, denoting the absence of ground state interaction.

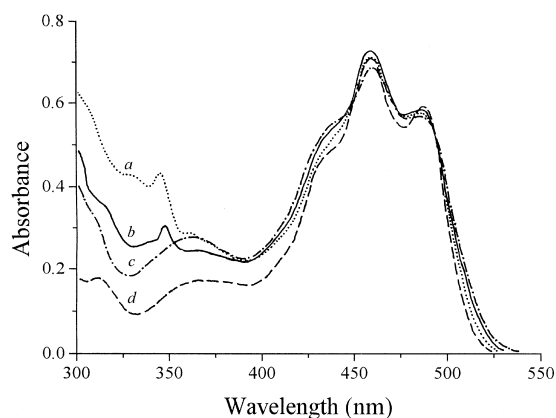


Fig. 3. Absorption spectra of the polyads containing viologen (a) tetrad **14**, (b) triad **13**, (c) dyad **11**, and model compound **2** (d) in methanol.

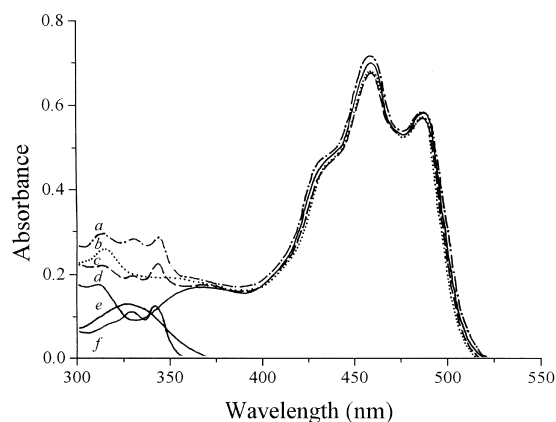


Fig. 4. Absorption spectra of the polyads containing no viologen (a) triad **12**, (b) dyad **10**, (c) dyad **9**, and model compounds (d) dibutyl derivative of fluorescein **2**, (e) 2-methyl-anthraquinone, (f) 9-butyl-carbazole in methanol.

3.3. Photoinduced intramolecular interaction in dyads

In the molecule of fluorescein, the phenyl group is almost perpendicular to the xanthene ring [13]. Previously [5,14], we have found that in polar sol-

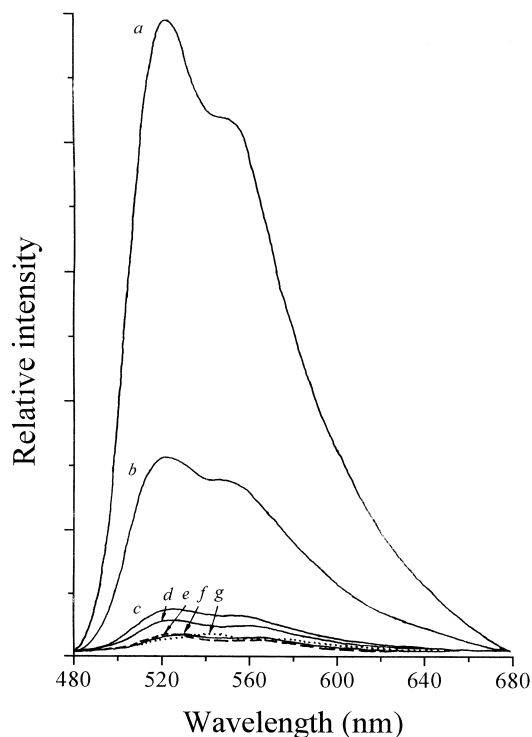


Fig. 5. Fluorescence spectra of model compound **2** (a), and polyads (b) dyad **10**, (c) dyad **9**, (d) triad **12**, (e) tetrad **14**, (f) triad **13**, (g) dyad **11** in methanol when fluorescein was excited at 460 nm.

Table 3
Photophysical properties of polyads and the model compound in methanol

Compound	Φ_F^a	τ_F/ns^b	Φ_Q^c	Φ_D^c	Φ_S^c	K_C^c
Model 2	0.35	2.63	—	—	—	—
Dyad 9	0.025	0.30	0.91	0.89	0.02	2.9
Dyad 10	0.14	1.41	0.60	0.46	0.14	0.6
Dyad 11	0.012	2.65	0.97	0	0.97	28.2
Triad 12	0.022	0.52 (98%)	0.94	0.80	0.14	—
	—	1.29 (2%)	—	—	—	—
Triad 13	0.0096	0.91 (87%)	0.97	0.65	0.32	—
	—	2.19 (13%)	—	—	—	—
Tetrad 14	0.0085	0.80	0.98	0.70	0.28	—

^a Φ_F is the fluorescence quantum yield of compounds.

^b τ_F is the fluorescence lifetime.

^c Φ_Q , Φ_D , Φ_S and K_C represent the total fluorescence quenching efficiency, dynamic quenching efficiency, static quenching efficiency and equilibrium constant of the intramolecular complex in polyads respectively.

vents the mutual orientation of the two chromophores in the dyads linked by a flexible butylene spacer at the carboxyl group of fluorescein is face-to-face to some degree, while that in the dyads linked at the hydroxyl group of fluorescein is shoulder-to-shoulder to some degree. The face-to-face orientation, as compared with the shoulder-to-shoulder, is the more favorable orientation between the two π -ring systems for photoinduced electron transfer.

In the dyad consisting of carbazole and fluorescein **9**, carbazole is linked at the carboxyl group of fluorescein, and thus the molecular conformation of dyad **9** is favorable for the photoinduced intramolecular electron transfer. When fluorescein is excited, Table 2 shows that the free energy change of the forward electron transfer (ΔG^f) from carbazole to fluorescein is -0.19 eV, indicating that electron transfer between the lowest excited state of fluorescein and the attached carbazole is feasible. Table 3 shows that the photoinduced intramolecular electron transfer efficiency is quite high ($\Phi_Q = 0.91$), and the electron transfer is mainly a dynamic process, denoting that carbazole is a very effective electron donor.

When fluorescein is excited in the dyad consisting of fluorescein and anthraquinone **10**, there occurs photoinduced intramolecular electron transfer from

fluorescein to anthraquinone ($\Delta G^f = -0.63$ eV, $\Phi_Q = 0.60$), and the electron transfer is also mainly a dynamic process. This implies that anthraquinone is an effective electron acceptor. However, the fluorescence quenching efficiency in dyad **10** is lower than that in dyad **9**, which may be explained that in dyad **10**, the anthraquinone moiety is linked at the hydroxyl group of fluorescein with a methylene group, so the two chromophores must adopt an angle around 109.5° . Such a relatively rigid molecular conformation is disadvantageous upon the intramolecular electron transfer.

In the dyad consisting of fluorescein and viologen **11**, when fluorescein is excited, the photoinduced intramolecular electron transfer from fluorescein to viologen is also feasible ($\Delta G^f = -1.15$ eV, $\Phi_Q = 0.97$). In fact, the dyad shows only the static process presumably resulting from the fact that viologen is positively double charged and therefore readily forms a non-emitting complex with fluorescein due to static electricity. From Table 3, it can be seen that in dyad **11** the equilibrium constant of the intramolecular complex formation is very high ($K_C = 28.2$).

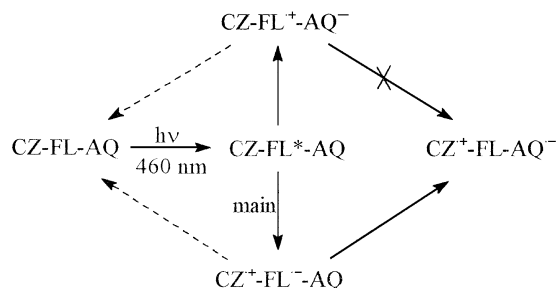
The free energy changes of the backward intramolecular recombination reaction in the dark (ΔG^r) in dyads **9**, **10**, **11** is -2.30 , -1.86 and -1.34 eV, respectively, indicating the recombination reactions in all three dyads is quite fast. In order to obtain the charge separated products with long lifetimes, we designed and synthesized the two triads **12** and **13**.

3.4. Photoinduced intramolecular electron transfer in triads

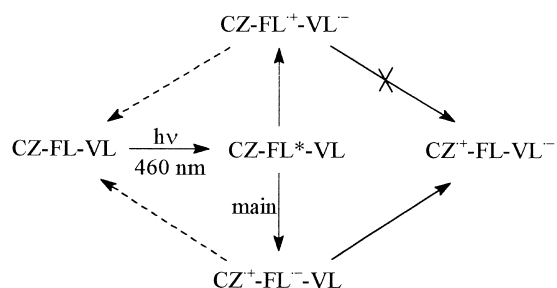
There is competition between the photoinduced intramolecular electron transfer reactions from carbazole to fluorescein ($\Delta G^f = -0.19$ eV) and from fluorescein to anthraquinone (in triad **12**, $\Delta G^f = -0.63$ eV) or viologen (in triad **13**, $\Delta G^f = -1.15$ eV) when fluorescein is excited in the triads. It is reasonable to assume that the mutual orientation of the chromophores in our triads, in which carbazole is always linked at the carboxyl group of fluorescein, is similar to that in dyads; thus in the primary charge separation

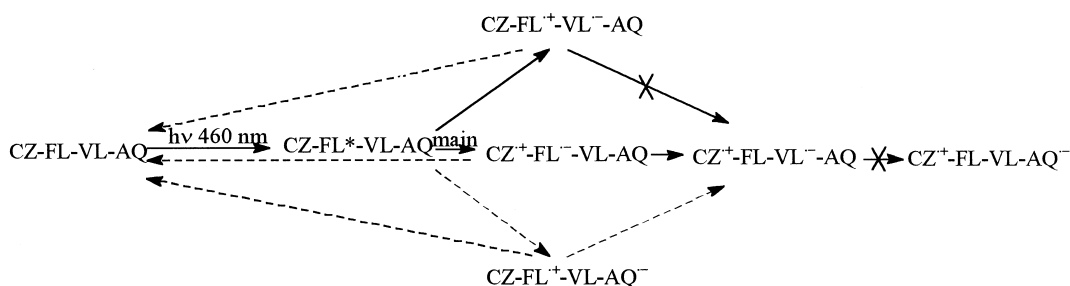
processes in triads, the electron transfer from carbazole to fluorescein should be predominant. The experimental results is concordant with this deduction. The triad consisting of carbazole, fluorescein and anthraquinone **12** (CZ-FL-AQ) exhibits two fluorescence lifetimes. One is 0.52 ns, which is close to that in dyad **9** (0.30 ns), covers a proportion of 98%. The other is 1.29 ns, which is similar to that in dyad **10** (1.41 ns), covers only 2%. This means that in triad **12**, the primary process in the main part is the electron transfer from carbazole to fluorescein when fluorescein is excited.

In triad **12**, when the initial photoinduced electron transfer proceeds between carbazole and fluorescein ($\text{CZ-FL-AQ} \rightarrow \text{CZ}^{\cdot+}\text{-FL}^{\cdot-}\text{-AQ}$), the next step in the formation of the final charge-separated state will be the electron transfer process from $\text{FL}^{\cdot-}$ to AQ ($\text{CZ}^{\cdot+}\text{-FL}^{\cdot-}\text{-AQ} \rightarrow \text{CZ}^{\cdot+}\text{-FL-AQ}^{\cdot-}$), which competes with the recombination reaction between carbazole and fluorescein ($\text{CZ}^{\cdot+}\text{-FL}^{\cdot-}\text{-AQ} \rightarrow \text{CZ-FL-AQ}$). Table 2 shows that the former is exergonic by $\Delta G^f = -0.24$ eV and the ΔG^r (-2.30 eV) of the latter is in the Marcus inverted region, so is restrained to some extent. This implies that the electron transfer from $\text{FL}^{\cdot-}$ to AQ is the predominant process. On the other hand, if the initial photoinduced electron transfer proceeds between fluorescein and anthraquinone ($\text{CZ-FL-AQ} \rightarrow \text{CZ-FL}^{\cdot+}\text{-AQ}^{\cdot-}$), the subsequent step will involve electron transfer from the cation radical of fluorescein to carbazole ($\text{CZ-FL}^{\cdot+}\text{-AQ}^{\cdot-} \rightarrow \text{CZ}^{\cdot+}\text{-FL-AQ}^{\cdot-}$), which will be thermodynamically inhibited ($\Delta G^f = 0.20$ eV), and thus the recombination reaction between fluorescein and anthraquinone will take place ($\Delta G^f = -1.86$ eV). After the formation of the final charge-separated state ($\text{CZ}^{\cdot+}\text{-FL-AQ}^{\cdot-}$), the recombination reaction between FL and $\text{AQ}^{\cdot-}$ is also thermodynamically inhibited ($\Delta G^f = 0.24$ eV). Based on the analysis above, it is reasonable to assume that in triad **12** a stable charge-separated state ($\text{CZ}^{\cdot+}\text{-FL-AQ}^{\cdot-}$) exists, which has a relatively large distance between the positive and negative charges and will slow down the charge recombination. The multistage electron transfer in triad **12** probably occurs as follows:



Similar to triad **12**, the triad consisting of carbazole, fluorescein and viologen **13** (CZ-FL-VL) also has two lifetimes, the lower of which is 0.91 ns, comparable with that of dyad **9** (0.30 ns), covering 87%; and the longer is 2.19 ns, near that of dyad **11**, covering 13%. It suggests that the electron transfer reaction between fluorescein and carbazole ($\Delta G^f = -0.19$ eV) is the predominant photoinitiated process when fluorescein is excited in triad **13**. After the primary electron transfer from carbazole to fluorescein, the secondary electron transfer from the anion radical of fluorescein to viologen can also take place ($\Delta G^f = -0.76$ eV), while the backward recombination process is thermodynamically inhibited ($\Delta G^r = 0.76$ eV). Therefore, at last a longer-lived charge-separated product ($\text{CZ}^{\cdot+}\text{-FL-VL}^{\cdot-}$) can be formed because the charge recombination here needs a longer path. In addition, after the initial photoinduced electron transfer from fluorescein to viologen ($\Delta G^f = -1.15$ eV), the electron transfer between carbazole and the cation radical of fluorescein cannot occur ($\Delta G^f = 0.20$ eV), and the charge recombination will easily take place ($\Delta G^r = -1.34$ eV). The probable multistage electron transfer in triad **13** is shown below.





3.5. Photoinduced intramolecular electron transfer in tetrad

In the tetrad consisting of carbazole, fluorescein, viologen and anthraquinone **14** (CZ-FL-VL-AQ), the fluorescence of fluorescein is quenched stronger than that in the triad **13**. When fluorescein is excited in tetrad **14**, there are three possible primary photoinduced intramolecular electron transfer processes viz., from carbazole to fluorescein ($\Delta G^f = -0.19$ eV); from fluorescein to viologen ($\Delta G^f = -1.15$ eV); from fluorescein to anthraquinone ($\Delta G^f = -0.63$ eV). According to the discussion about the primary electron transfer process in triads, we assume that the electron transfer from carbazole to fluorescein is the predominant primary process. The electron transfer processes between carbazole, fluorescein and viologen in tetrad **14** is similar to those in triad **13**. From Table 2, we can see that the electron transfer from VL $^{\cdot-}$ to AQ is ruled out ($\Delta G^f = 0.52$ eV), while the electron transfer from AQ $^{\cdot-}$ to VL is thermodynamically permitted ($\Delta G^f = -0.52$ eV). Therefore, in tetrad **14**, the final longer-lived charge-separated product is CZ $^{\cdot+}$ -FL-VL $^{\cdot-}$ -AQ. The possible multistage electron transfer in triad **14** is shown above.

4. Conclusion

In all of our polyads containing fluorescein as photosensitizer, carbazole as electron donor, viologen and anthraquinone as electron acceptors, the fluorescence of fluorescein is strongly quenched in methanol. The quenching by carbazole and anthraquinone is dominantly a dynamic electron transfer process, while viologen easily forms a

non-emitting complex with fluorescein in polyads, probably due to its double positive charges. When fluorescein in the triads and tetrads is excited, the primary photoinduced intramolecular electron transfer process is mainly electron transfer from carbazole to fluorescein. Estimated results of the free energy changes of electron transfer reactions indicate that in the triads and tetrads, after the initial charge separation, the subsequent electron transfer processes can occur, and longer-lived charge-separated products can be then obtained.

Acknowledgements

The authors are grateful to the National Natural Science Foundation of China for financial support (no. 59783007).

References

- [1] Gust D, Moore TA. Mimicking of photosynthetic electron and energy transfer. *Adv Photochem* 1991;16:1–66.
- [2] Neckers DC, Valdes-Aguilers OM. Photochemistry of xanthene dyes. *Adv Photochem* 1995;18:315–94.
- [3] Zhao Z, Shen T, Xu H. Photoinduced interaction between eosin and viologen. *J Photochem Photobiol A: Chem* 1990;52:47–53.
- [4] Sun L, Yang Y, He J, Shen T. Fluorescence quenching of viologen on xanthene dyes in dyads. *Dyes and Pigments* 1995;28:275–9.
- [5] Zhang H, Zhang M, Shen T. Photoinduced intramolecular electron transfer between fluorescein and carbazole. *Science in China B* 1997;40:192–8.
- [6] Hiroshi I, Atsuhiko N, Tomio T, Hideo K. A manufacturing method of halo-substituted amino compounds. *Jpn Kokai Tokyo Koho JP 61 180 726* [86 180 726], 1986 (Chem Abstr 1987;(106);50036).
- [7] Bhavsar MD, Tilak BD, Venkataraman K. Anthraquinone and anthrone series. XXI. 2-(Bromomethyl)anthraquinones and their derivatives. *J Sci Ind Res* 1957;16B:392–9.

- [8] Shen T, Zhao Z, Yu Q, Xu H. Photosensitized reduction of benzil by heteroatom-containing anthracene dyes. *J Photochem Photobiol A: Chem* 1989;47:203–12.
- [9] Kararnos GF, Tarro NJ. Photosensitization by reversible electron transfer: theories, experimental evidence, and examples. *Chem Rev* 1986;86:401–49.
- [10] Schmidt JA, McIntosh AR, Weedon AC, Bolton JR, Connolly JS, Hurley JK, Wasielewski MR. Intramolecular photochemical electron transfer. 4. Singlet and triplet mechanisms of electron transfer in a covalently linked porphyrin-amide-quinone molecule. *J Am Chem Soc* 1988;110:1733–40.
- [11] Falkner LR, Tachikawa H, Bard AJ. Electrogenerated chemiluminescence. VII. The influence of an external magnetic field on luminescence intensity. *J Am Chem Soc* 1972;94:691–9.
- [12] Zhou Q, Shen S, Yuan Z, Zhou Y, Shen T. Effect of excitation wavelength on photophysics of fluorescein-antracene-methyl ester. *J Photochem Photobiol A: Chem* 1990;51:229–35.
- [13] Osborn S, Rogers D. The crystal and molecular structure of the 1:1 complex of acetone with the lactoid form of fluorescein. *Acta Crystallogr Sect B* 1975;31:359–64.
- [14] Yu Q, He J, Shen T. Photoinduced singlet interactions between esters of xanthene dyes and anthroic acid. *J Photochem Photobiol A: Chem* 1996;97:53–6.